Cell-Membrane Imaging

DOI: 10.1002/ange.201205940

A Switchable Two-Photon Membrane Tracer Capable of Imaging Membrane-Associated Protein Tyrosine Phosphatase Activities**

*Lin Li, Xiaoqin Shen, Qing-Hua Xu, and Shao Q. Yao**

The plasma membrane is involved in a variety of important cellular processes such as cell adhesion and cell signaling, most of which are orchestrated by proteins embedded within its lipid bilayer. It is estimated that proteins occupy approximately 50% of a typical membrane volume, and in mammalian cells, more than one third of all genes encode membrane proteins of different functions.[1] Protein tyrosine phosphatases (PTPs) are signaling enzymes that remove the phosphate group from their protein substrates. One of the most important subclasses of PTPs is the membrane-associated, receptor-like protein tyrosine phosphatases (RPTPs), which are responsible for most of the protein phosphatase activities localized near the plasma membrane.[2] Dysregulation of PTPs, especially RPTPs, has been implicated in a variety of human diseases including cancer, diabetes, and autoimmune disorders.[3] Elevated levels of endogenous RPTP activities are well documented to be closely associated with tumorigenesis in numerous cells and tissues. Effective methods to fluorescently label the plasma membrane of cancer cells and tissues, as well as monitor membrane-localized RPTP activities, are therefore of significant interest in cell signaling and PTP biology. At present, few biochemical techniques are available for such labeling owing to the difficulty in working with membrane proteins.[4]

In recent years, biological and chemical approaches to study endogenous PTP expression and enzymatic activity have been developed.[5] Among them, imaging-based approaches are highly desirable because of their high sensitivity and good cellular resolution.[6] For example, Bastiaens and co-workers used a genetically encoded PTP biosensor based on Förster resonance energy transfer (FRET) to study the endogenous distribution of active PTPs.[7a] We and others have focused on small-molecule-based probes capable of imaging PTP enzymatic activities in cells and deep tissues.[7b–d] Despite the numerous desirable properties of small-molecule probes (for example, cell permeability, photophysical properties, chemical tractability, and others), many of them work well with cell lysates or fixed cells/tissues but are not suitable for live-cell imaging experiments owing to rapid diffusion of the dephosphorylated fluorescent product, which results in poor image resolution.[8] This problem could be alleviated in situ by introduction of reactive handles, cell-penetrating peptides (CPPs), or self-immobilizing components in the probe design.[7b,c,9] Herein, we report a very different design concept to achieve live-cell and deep-tissue imaging of membrane-associated RPTP activity using two-photon fluorescence microscopy (TPFM).

Two-photon (2P) fluorescence microscopy provides key advantages over conventional one-photon (1P) imaging techniques, namely, increased penetration depth, lower tissue autofluorescence and self-absorption, and reduced photodamage and photobleaching, and therefore is particularly useful for imaging deep tissues and animals.[6c,10] However, few 2P probes are available for live-cell and tissue imaging of enzymatic activities. To develop a system capable of imaging endogenous RPTP activities, it must possess two essential properties. First, the system must be a good 2P membrane tracer, giving a highly fluorescent signal only when it is localized/anchored to the plasma membrane of mammalian cells. Second, the fluorescence of the system must be switchable by endogenous RPTP activity. Although a number of membrane tracers are commercially available (Figure 1A), none of them possess acceptable 2P photophysical properties.[11] Previously, Cho and co-workers reported 2P probes based on hydrophobic aminonaphthalene dyes for the detection of lipid rafts and near-membrane calcium ions.[12] These probes, however, could not be easily converted into enzyme-detecting sensors. Belfield and co-workers recently reported a 2P-absorbing fluorene derivative, **LT1**, for selective lysosomal imaging in HCT 116 cancer cells (Figure 1B).[13] **LT1** contains a π-conjugated fluorene that is an excellent 2P reporter, and a pair of ten-unit poly(ethylene glycol) (PEG) groups for cellular uptake and selective lysosomal localization. Inspired by this finding, we designed **Flu7** (Figure 1C; boxed), which contains the π-conjugated fluorene moiety modified with two six-carbon aliphatic chains as a 2P reporter. We anticipated that the hydrophobic tails in **Flu7** could serve as membrane anchors, thus making it an excellent 2P membrane tracer. To achieve RPTP-responsive ON/OFF fluorescence in **Flu7**, we also replaced the two PEG groups in **LT1** with a pair of six-carbon groups containing positively charged, quaternary ammonium head groups. In addition, a pairing partner, **Q12**, which contains a "photocaged" phosphorylated phenolic group coupled to a fluorescence quencher (Disperse Red 1), was introduced.[14] With the **Flu7**/**Q12** system (Figure 1C), in the first step, **Flu7** can be used as

[*] Dr. L. Li, X. Shen, Prof. Dr. Q.-H. Xu, Prof. Dr. S. Q. Yao
Department of Chemistry
National University of Singapore
3 Science Drive 3, Singapore 117543 (Singapore)
E-mail: chmyaosq@nus.edu.sg
Homepage: http://staff.science.nus.edu.sg/~syao

[**] Funding was provided by the Agency for Science, Technology and Research (R-143-000-391-305) and the Ministry of Education (R-143-000-394-112). We also acknowledge the generous donation of Drosophila tissues from Dr. Kah-Leong Lim and Dr. Chengwu Zhang (NUS).

Supporting information for this article (experimental details) is available on the WWW under http://dx.doi.org/10.1002/anie.201205940.

WILEY ONLINE LIBRARY
© 2013 Wiley-VCH Verlag GmbH & Co. KGaA, Weinheim

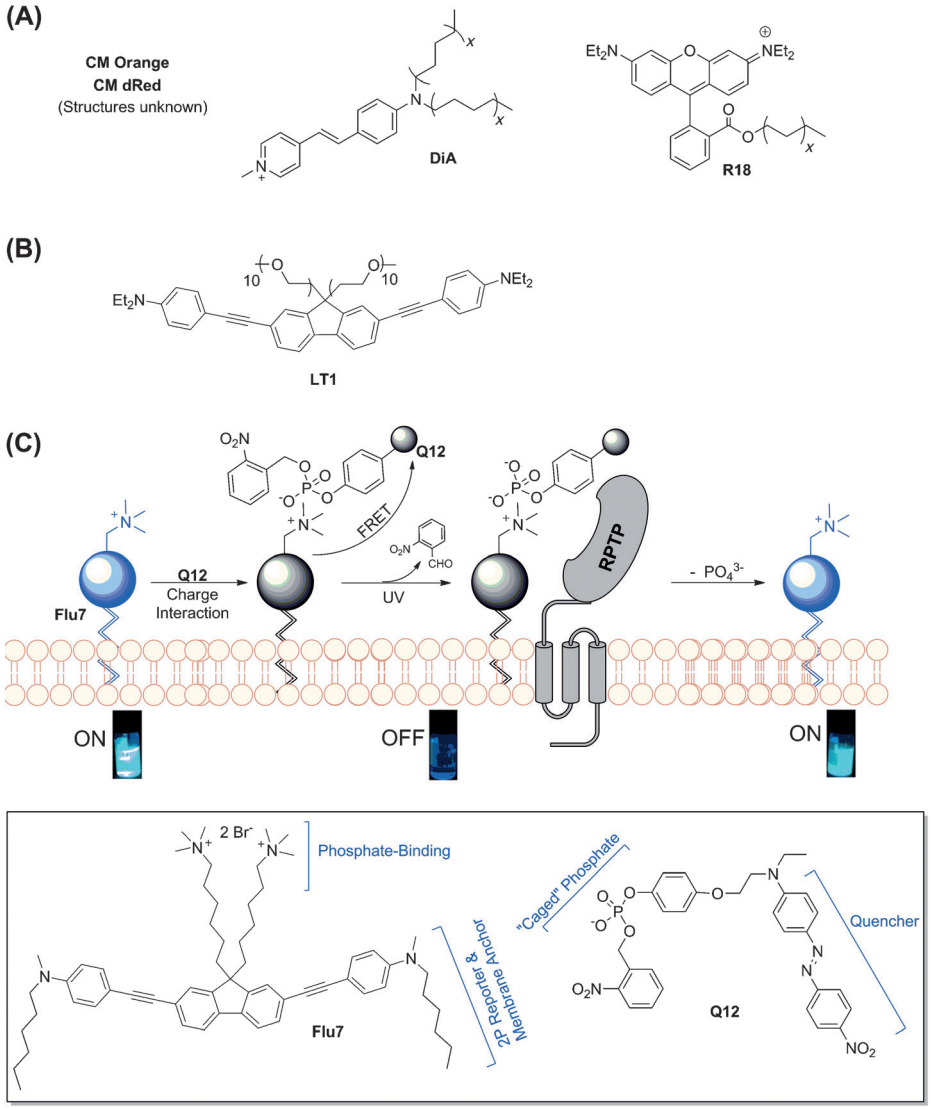

Figure 1. A) Commercially available membrane tracers, all of which have poor 2P properties. B) Previously reported 2P lysosomal tracer **LT1**. C) Overall strategy of our switchable 2P membrane tracer pair, **Flu7**/**Q12** (formulas shown in box), that is capable of imaging membrane-associated RPTP activity.

a 2P membrane tracer to stain the plasma membrane, producing what we call a "memory effect", which provides a suitable internal fluorescence standard of the cell for subsequent analysis of RPTP activities (ON state). Next, **Q12** can be added, and through electrostatic interactions, the negatively charged, caged phosphate group in **Q12** would bind to the positively charged **Flu7** head groups, thus effectively quenching its fluorescence through intermolecular FRET (OFF state). Using UV irradiation, the 2-nitrobenzyl group in **Q12** can be removed, exposing its uncaged phosphate, which can subsequently undergo enzymatic dephosphorylation by membrane-associated RPTPs. Finally, the dephosphorylated **Q12** would dissociate from **Flu7**, restoring its fluorescence (ON state). In essence, by taking advantage of the electrostatic interaction between **Flu7** and **Q12**, our strategy can achieve switchable ON/OFF/ON imaging of RPTP activity. It should be noted that FRET-based "turn-ON" sensors based on electrostatic interactions have previously been used for biological detection with conjugated polymers (CPs).[15] Our study represents the first small-molecule probes capable of 2P bioimaging of enzymatic activity in live cells using such design principles. For the synthesis of **Flu7**/**Q12**, previously published procedures were adopted with the necessary modifications (see Supporting Information for details).[13,14]

To demonstrate the potential utility of **Flu7** as a suitable standalone TPFM membrane tracer for live-cell imaging, we first evaluated its chemical, photophysical, and biological properties. Commercially available membrane tracers, including CellMask Orange, CellMask Deep Red, DiA, and R18, were used as references (Table 1, Figure 2, and Supporting Information). The absorption and emission spectra of **Flu7** were shown to be highly sensitive to solvent polarity, and the emission spectra exhibited large bathochromic shifts in the order of benzene < THF < DCM < ethanol < acetone < DMSO (Supporting Information, Figure S1). The emission spectra showed much greater solvatochromic shifts than the absorption spectra (56 nm versus 8 nm), suggesting that **Flu7** might be used as a polarity-sensitive probe. A similar outcome was observed with time-resolved fluorescence spectra. As shown in Table 1, under

Table 1: Photophysical data of **Flu7** and other commercially available membrane tracers.[a]

Probe	$\lambda_{abs}/\lambda_{fl}$[b]	ε (x10^3)[c]	$\Delta\gamma$[d]	Φ[e]	$\varepsilon\Phi$	$\delta\Phi$[f]
Flu7	398/471	45	3894	0.56	25 200	338
CM Orange	554/569	113	475	0.070	7910	0.84
CM dRed	655/673	269	408	0.020	5380	0.35
DiA	463/578	26	4297	0.089	2314	6.23
R18	562/585	159	699	0.11	17490	17.5

[a] All measurements were done in HEPES buffer (pH 7.5) with 0.02% Triton X-100. [b] Peak position of the longest absorption/emission band in nm. [c] Extinction coefficient in $M^{-1}cm^{-1}$. [d] Stokes shift in cm^{-1}. [e] Quantum yields determined by using fluorescein in aqueous NaOH (pH 13) as a standard. [f] The maximum 2P action cross-section values upon excitation from 750 nm to 840 nm in GM (1 GM = 10^{-50} cm^4 s photon^{-1}).

© 2013 Wiley-VCH Verlag GmbH & Co. KGaA, Weinheim

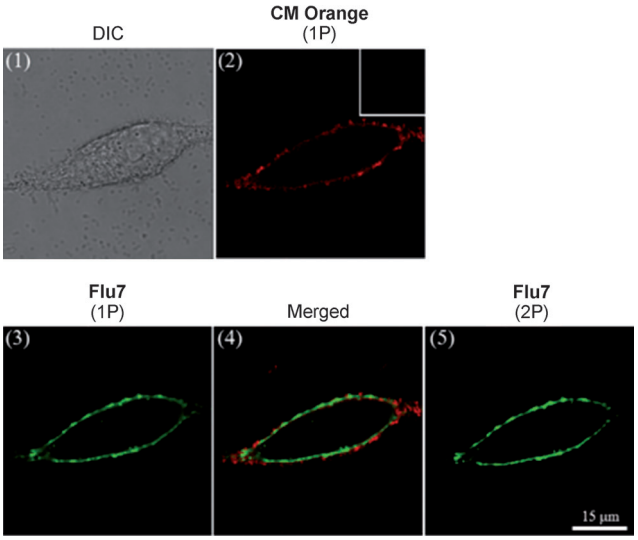

Figure 2. One- and two-photon excited fluorescence images of live HeLa cells upon staining with 0.25 μM **Flu7** for 30 min at 37 °C. 1) Differential interference contrast (DIC) image. 2) 1P image of cells stained with CM Orange (λ_{ex} = 543 nm, λ_{em} = 555–650 nm). Inset: 2P image of the same cell. 3, 5) 1P (λ_{ex} = 405 nm, λ_{em} = 430–530 nm) and 2P (λ_{ex} = 770 nm, λ_{em} = 430–530 nm) images, respectively, of cells stained with **Flu7**. 4) Merged image of (2) and (3).

physiological, membrane-like conditions (HEPES buffer, pH 7.5, 0.02 % Triton X-100), **Flu7** had maximum absorption and emission bands at 398 nm and 471 nm, respectively. Its fluorescence properties (see Table 1 for definitions; ε = 45 000 $M^{-1}cm^{-1}$, Φ = 0.56, giving $\varepsilon\Phi$ = 25 200) were largely independent of pH changes (Figure S7), and with a high 2P action cross-section ($\delta\Phi$ = 338 GM), **Flu7** was indeed an excellent 2P dye that was excited by a common two-photon laser. Without Triton X-100, **Flu7** showed 37-fold lower brightness ($\varepsilon\Phi$ = 646; see Table S2), indicating the fluorescence of **Flu7** could be selectively turned ON when localized to membrane-like environments. In contrast, all commercial membrane tracers showed significantly weaker fluorescence ($\varepsilon\Phi$ = 2314–17 490) and much smaller 2P action cross-sections ($\delta\Phi$ = 0.35–17.5 GM) under the conditions tested (Table 1), making them unsuitable for TPFM (Figure S4). Both the photostability and cell toxicity of **Flu7** were shown to compare favorably with known membrane tracers (Figure S2 & S3), making it suitable for live-cell imaging. Indeed, when live HeLa cancer cells were treated with **Flu7**, followed by one- or two-photon fluorescence microscopy, we observed fluorescent staining exclusively within the plasma membrane of the cells (Figure 2). Prolonged incubation of the cells with **Flu7** did not lead to staining of other lipid-like environments in intracellular organelles (for example, the ER membrane) indicating minimal probe internalization, which confirms **Flu7** is plasma-membrane specific. Independent experiments using membrane fractionation further validated this finding (Figure S5).

We next investigated whether **Flu7**/**Q12** work as a turn ON/OFF/ON system for imaging membrane-associated RPTP activity. As shown in Figure 3 A, titration of **Q12** to **Flu7** in HEPES buffer (pH 7.5, 0.02 % Triton X-100) led to a dose-dependent decrease in **Flu7** fluorescence intensity, with nearly complete quenching of fluorescence detected at 1 equiv. of **Q12**, indicating the formation of a 1:1 **Flu7**/**Q12** complex and efficient intermolecular FRET (OFF). The titration curves were fitted to a 1:1 binding model to obtain both the dissociation and Stern–Volmer constants of the complex ($K_d = 1.54 \pm 0.32 \times 10^{-7}$ M; $K_{SV} = 5.24 \pm 0.63 \times 10^6\,M^{-1}$). Nearly identical results were observed for the 2P process (Figure S6, S7). Titration between the control compound **Flu15** (which contains only one of the quaternary ammonium head groups) and **Q12** was similarly carried out; results showed nearly identical K_d and K_{SV} ($1.77 \pm 0.25 \times 10^{-7}$ & $5.01 \pm 0.71 \times 10^6\,M^{-1}$; Figure S7), indicating that one positively charged quaternary ammonium group was sufficient for tight binding and fluorescence quenching by **Q12**. The non-phosphorylated version of the quencher **Q14** did not bind to **Flu7**, nor did it quench its fluorescence. Next, the **Flu7**/**Q12** pair was subjected to competition from ten equivalents of common biological anions (Figure 3 B); none of the anions tested showed any noticeable effect on **Flu7**/**Q12** fluorescence. This result indicates that the association of **Flu7**/**Q12** was driven not only by electrostatic interactions, but also by other non-covalent interactions (for example, π–π stacking and hydrophobic interactions). Minimal interference from these biological analytes ensures that our system could work well in live cells and tissues. We next established that **Q12** was completely uncaged following UV irradiation of 500 μJ cm^{-2} for three minutes and dephosphorylated by recombinant PTP1B (an important mammalian PTP involved in diabetes and obesity[16]) within 90 minutes, using an HPLC assay (Figure S8). Time-dependent fluorescence measurements from UV-irradiated **Flu7**/**Q12** (1:1) pair treated with PTP1B also showed a concomitant increase in fluorescence (Figure 3 C), with nearly complete recovery of fluorescence within 120 minutes (ON). These data were fitted to give an apparent second-order rate constant of $k_{app} = 2.30 \pm 0.35 \times 10^4\,M^{-1}s^{-1}$ for the enzyme-catalyzed dephosphorylation step. Having successfully demonstrated the enzyme-controlled, ON/OFF/ON switching of our system under in vitro conditions, we next carried out live-cell-imaging experiments (Figure 3 D). Similar to Figure 2, upon treatment with **Flu7**, images of the membrane-stained cells were quantified and used as an internal reference (ON state). Subsequently, **Q12** was added, followed by cell washing and imaging. Complete fluorescence quenching of the stained membrane was observed (OFF state). Upon UV irradiation, the cells were imaged in real-time over the course of 120 minutes (the 60 minute image is shown in Figure 3 D, panel 3); a gradual increase in fluorescence over the whole cell was observed, with saturation at 120 minutes (Figure 3 E). Fractionation of plasma membranes from the treated cells further confirmed that the switchable nature of the **Flu7**/**Q12** system was indeed membrane-selective, UV dependent, and enzyme-activity dependent.

Because our **Flu7**/**Q12** system provides a simple and rapid means to selectively measure membrane-associated endogenous RPTP activity in live cells, we next investigated whether it could be used to differentiate the elevated activity of RPTP found in many cancer cell lines. The clear advantages of the

 © 2013 Wiley-VCH Verlag GmbH & Co. KGaA, Weinheim

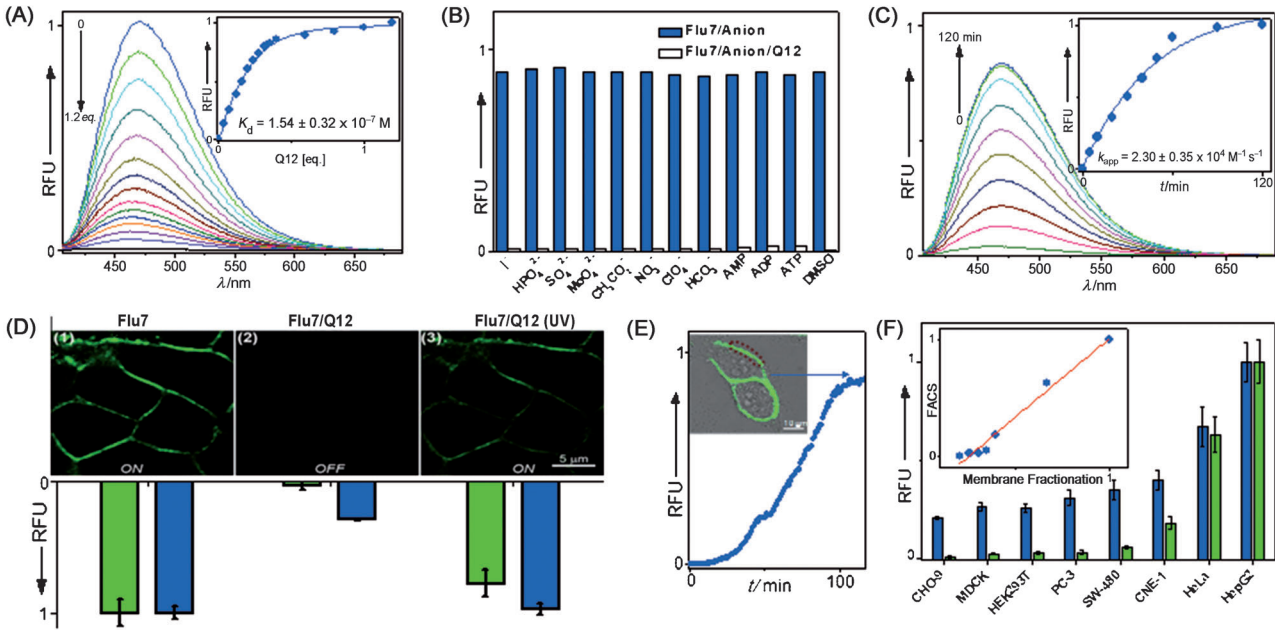

Figure 3. A) 1P excited fluorescence emission spectra of 1.0 μM **Flu7** in HEPES buffer (pH 7.5; supplemented with 0.05 M NaCl, 2.5 mM EDTA, 2 mM DTT, and 0.02% Triton X-100) after addition of **Q12** (0–1.2 equiv.). Inset: fitted curve of K_d values. B) Effect of anions (10 equiv.) on **Flu7**/**Q12** fluorescence. C) Time-dependent 1P fluorescence spectra of **Flu7**/uncaged **Q12** upon treatment with PTP1B over the course of 120 min. PTP1B/probe ratio = 1:40. Inset: fitted curve of k_{app}. D) 1P fluorescence images of HepG2 cells treated successively with **Flu7** (1), **Q12** (2), and UV irradiation (3). Bottom: the total fluorescence intensity of the images was quantified and plotted (green). For comparison, membrane fractions of the same treated cells were isolated, resolubilized, fluorescently quantified, and plotted (blue). E) Time-dependent fluorescence changes of live HeLa cells treated with **Flu7**/**Q12** followed by 2 min UV irradiation. The cells were subsequently imaged over the course of 120 min at 60 s intervals (λ_{ex} = 405 nm, λ_{em} = 430–530 nm). The image shown was taken at 100 min. F) Membrane-associated RPTP activity of eight different mammalian cell lines measured by FACS (green) and membrane fractionation (blue) experiments. For FACS, cells were treated with **Flu7**/**Q12**, UV-irradiated, then sorted. For membrane fractionation, membranes of untreated cells were isolated, resolubilized, and treated with DiFMUP to measure phosphatase activity. Inset: correlation between these two experiments, fitted by linear regression, giving R^2 = 0.98. RFU = relative fluorescence units.

present system over other phosphatase-detecting systems (such as ELF 97) are its compatibility with live cells and its ability to focus on only membrane-associated activity (thus, making it less susceptible to interference from cytosolic phosphatases). A total of eight mammalian cell lines were used, three of which were normal cell lines (CHO-9, MDCK, and HEK293T) and the rest were cancer cell lines (PC-3, SW-480, CNE-1, HeLa, and HepG2). In addition, membrane-fractionation experiments were carried out, in which plasma membranes of each of the eight cell lines were isolated, resolubilized, and treated with DiFMUP (to measure endogenous membrane-associated phosphatase activity; Figure 3F). Independently, cells treated with **Flu7**/**Q12** followed by UV irradiation were imaged (Figure S12) and the eight cell lines could readily be grouped into strong (HepG2, HeLa), medium (CNE-1, SW-480), and weak (PC-3, HEK293T, MDCK, CHO-9) groups, based on their membrane-associated RPTP activity. Flow-cytometric analysis was carried out to further quantify the relative fluorescence of these cells and compared with the membrane fractionation results (Figure 3F); a good correlation was obtained between the FACS and fractionation results.

Finally, to establish the utility of our system in TPFM, we imaged membrane-associated RPTPs activity deep inside live *Drosophila* brains. Upon incubation with 20 μM of **Flu7** for two hours at room temperature, the brain of a one-day-old female *Drosophila* was imaged at a depth of approximately 110 μm (Figure 4); these images revealed fluorescent membrane staining mostly in the medulla region of the brains. Upon further incubation with UV-irradiated **Q12**, the fluorescence signals were initially quenched (panel 3), but slowly recovered to near full intensity over the next six hours (panel 4). This much deeper penetration, coupled with

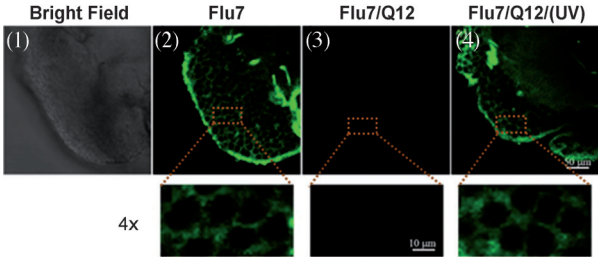

Figure 4. 2P imaging of RPTP activity in the brain of a one-day-old live female *Drosophila* using **Flu7**/**Q12**. The images were taken at λ_{ex} = 770 nm at a depth of ca. 110 μm with 63× magnification (λ_{em} = 430–530 nm). 1) Bright-field image. 2) Image after 2 h treatment with **Flu7** (20 μM). 3) Image after 20 min incubation with uncaged **Q12** (100 μM). 4) Image of (3) after another 6 h incubation. Bottom: 4× magnification of the boxed regions.

© 2013 Wiley-VCH Verlag GmbH & Co. KGaA, Weinheim

significantly lower background fluorescence in the TPFM images when compared to 1P techniques, clearly demonstrated the potential of our strategy for use in future tissue and animal experiments.

In conclusion, we have developed a switchable two-photon membrane tracer capable of imaging membrane-associated protein tyrosine phosphatase activity. The ON/OFF/ON feature of this strategy is a direct result of a reversible **Flu7**/**Q12** electrostatic interaction, modulated by both UV light and enzyme catalysis. The ability to selectively image localized phosphatase activity in live cells was used to quantify endogenous levels of RPTP activity in different mammalian cells without physical separation of the plasma membranes. Given the fact that most membrane-associated phosphatases in mammalian cells are PTPs, we made an assumption that most of the membrane-associated phosphatase activity detected in our probe system was from RPTPs. An important unresolved issue from the current study is the lack of selectivity of our probe system from other endogenous non-PTP phosphatase activities.

Received: July 25, 2012
Published online: October 4, 2012

Keywords: bioimaging · fluorescence microscopy · membrane proteins · phosphatases · small-molecule probes

[1] H. Lodish, A. Berk, S. L. Zipursky, P. Matsudaira, D. Baltimore, J. Darnell, *Molecular Cell Biology*, New York, Scientific American Books, 4th ed., **2004**.
[2] N. K. Tonks, *Nat. Rev. Mol. Cell Biol.* **2006**, *7*, 833 – 846.
[3] A. Östman, C. Hellberg, F. D. Böhmer, *Nat. Rev. Cancer* **2006**, *6*, 307 – 320.
[4] a) V. V. Vintonyak, A. P. Antonchick, D. Rauh, H. Waldmann, *Curr. Opin. Chem. Biol.* **2009**, *13*, 272 – 283; b) C. H. S. Lu, K. Liu, L. P. Tan, S. Q. Yao, *Chem. Eur. J.* **2012**, *18*, 28 – 39.
[5] a) S. Liu, B. Zhou, H. H. Yang, Y. He, Z. X. Jiang, S. Kumar, L. Wu, Z. Y. Zhang, *J. Am. Chem. Soc.* **2008**, *130*, 8251 – 8260; b) S. Mizukami, S. Watanabe, K. Kikuchi, *ChemBioChem* **2009**, *10*, 1465 – 1468; c) A. Nören-Müller, W. Wilk, K. Saxena, H. Schwalbe, M. Kaiser, H. Waldmann, *Angew. Chem.* **2008**, *120*, 6061 – 6066; *Angew. Chem. Int. Ed.* **2008**, *47*, 5973 – 5977; d) K. A. Kalesh, L. P. Tan, K. Liu, L. Gao, J. Wang, S. Q. Yao, *Chem. Commun.* **2010**, *46*, 589 – 591.
[6] a) R. Y. Tsien, *Angew. Chem.* **2009**, *121*, 5721 – 5736; *Angew. Chem. Int. Ed.* **2009**, *48*, 5612 – 5626; b) F. Helmchen, W. Denk, *Nat. Methods* **2005**, *2*, 932 – 940.
[7] a) I. A. Yudushkin, A. Schleifenbaum, A. Kinkhabwala, B. G. Neel, C. Schultz, P. I. H. Bastiaens, *Science* **2007**, *315*, 115 – 119; b) M. Hu, L. Li, H. Wu, Y. Su, P. Y. Yang, M. Uttamchandani, Q. H. Xu, S. Q. Yao, *J. Am. Chem. Soc.* **2011**, *133*, 12009 – 12020; c) L. Li, J. Ge, H. Wu, Q. H. Xu, S. Q. Yao, *J. Am. Chem. Soc.* **2012**, *134*, 12157 – 12167; d) ELF 97 is a commercial phosphatase detection dye commonly used to image endogenous phosphatase activities in fixed cells and tissues. This compound however is not cell-permeable and cannot be used for live-cell imaging.
[8] A. Baruch, D. A. Jeffery, M. Bogyo, *Trends Cell Biol.* **2004**, *14*, 29 – 35.
[9] a) G. Blum, S. R. Mullins, K. Keren, M. Fonovic, C. Jedeszko, M. J. Rice, B. F. Sloane, M. Bogyo, *Nat. Chem. Biol.* **2005**, *1*, 203 – 209; b) D. H. Kwan, H. M. Chen, K. Ratananikom, S. M. Hancock, Y. Watanabe, P. T. Kongsaeree, A. L. Samuels, S. G. Withers, *Angew. Chem.* **2011**, *123*, 314 – 317; *Angew. Chem. Int. Ed.* **2011**, *50*, 300 – 303; c) J. Ge, L. Li, S. Q. Yao, *Chem. Commun.* **2011**, *47*, 10939 – 10941.
[10] a) M. Pawlicki, H. A. Collins, R. G. Denning, H. L. Anderson, *Angew. Chem.* **2009**, *121*, 3292 – 3316; *Angew. Chem. Int. Ed.* **2009**, *48*, 3244 – 3266; b) H. M. Kim, B. R. Cho, *Chem. Commun.* **2009**, 153 – 164.
[11] http://www.invitrogen.com. Both CM Orange and CM dRed are proprietary compounds whose structures are not disclosed by the vendor.
[12] a) H. M. Kim, B. R. Kim, H. J. Choo, Y. G. Ko, S. J. Jeon, C. H. Kim, T. Joo, B. R. Cho, *ChemBioChem* **2008**, *9*, 2830 – 2838; b) C. S. Lim, H. J. Kim, J. H. Lee, Y. S. Tian, C. H. Kim, H. M. Kim, T. Joo, B. R. Cho, *ChemBioChem* **2011**, *12*, 392 – 395.
[13] X. Wang, D. M. Nguyen, C. O. Yanez, L. Rodriguez, H. Y. Ahn, M. V. Bondar, K. D. Belfield, *J. Am. Chem. Soc.* **2010**, *132*, 12237 – 12239.
[14] C. J. Zhang, L. Li, G. Y. J. Chen, Q. H. Xu, S. Q. Yao, *Org. Lett.* **2011**, *13*, 4160 – 4163.
[15] a) X. Feng, L. Liu, S. Wang, D. Zhu, *Chem. Soc. Rev.* **2010**, *39*, 2411 – 2419; b) N. Tian, Q. H. Xu, *Adv. Mater.* **2007**, *19*, 1988 – 1991.
[16] T. O. Johnson, J. Ermolieff, M. R. Jirousek, *Nat. Rev. Drug Discovery* **2002**, *1*, 696 – 709.

 © 2013 Wiley-VCH Verlag GmbH & Co. KGaA, Weinheim